

EVALUATION OF THE FENTON HILL HOT DRY ROCK
GEOTHERMAL RESERVOIR

PART II. FLOW CHARACTERISTICS AND GEOCHEMISTRY

Charles O. Grigsby
Jefferson W. Tester

Flow Impedance

For the circulation system, the flow impedance is defined as the pressure drop through the fracture system connecting the production and injection wellbores divided by the production flow rate. Figure II-1 shows the measured impedance corrected for buoyancy effects between the cold and hot well bores. The large decrease in impedance is attributed to changes in the fracture system and its connections to the wellbores caused by localized cooling (thermal stress) and/or pore pressure induced "stress relief" effects. Changes in impedance have been attributed to shear-like, discrete events occurring within the reservoir. These changes are apparently irreversible and indicate that the rock may have undergone considerable dislocation during the flow test.

Fracture Volume and Degree of Mixing

Dye tracer techniques developed previously were used to characterize the fracture system volume under flow conditions and the fluid residence-time distribution (RTD) within the reservoir.¹ In the four experiments run during the 75-day test, a 200 ppm, 100 gal (400 liter) pulse of sodium-fluorescein dye was injected into the EE-1 wellhead, pumped down EE-1 and through the fractured region, and up the GT-2B wellbore. Dye concentration in the produced fluid was monitored spectrophotometrically at the surface as a function of time and volume throughput. The results of the four experiments are described by plotting normalized tracer concentration as a function of effective fracture system or throughput volume as shown in Fig. II-2.

Flow in the fracture system can be described as well-mixed with no major short circuits. The degree of mixing cannot be adequately accounted for by dispersion of flow in a single hydraulic fracture. Because of this fact and of the known existence of multiple flow paths between EE-1 and GT-2B, the observed shape of the RTD is caused by dispersion within individual flow paths as well as superposition from mixing of various production flows in the wellbore. Consequently, several statistical quantities are needed to

describe flow in the system. The median volume reasonably represents the flow through the major production paths in GT-2B while the increase in the spread of the distribution is indicative of longer residence time paths possibly through more circuitous routes in the rock.

Several general comments can be made: (1) the fracture flow system has grown considerably in size during the 75-day test, the integrated mean fracture system volume was 14,900 gal on 4/7/78, up from 9090 on 2/9/78 and the median volume is larger, 12,800 gal versus 6750 gal, (2) there is evidence for the development of additional secondary flow paths, that is the tendency toward earlier and later arrival of dye with smaller and larger residence times (or volumes) causing an increase in the spread of the distribution, (3) the apparent degree of mixing or dispersion is virtually unchanged between the 3/1/78 and 4/7/78 experiments as shown by the similar shapes of the phase 1-2, 1-3, and 1-4 curves when plotted on normalized volume coordinates.

Fluid Geochemistry

Samples of the circulating fluid were collected periodically at the injection wellhead, the production wellhead, and from the makeup system. A mass balance of dissolved material in the fluid circulating through the surface system indicates that no deposition or scaling occurred in the surface equipment. The change in concentration with time of various dissolved species in the recirculating fluid should be consistent with the models which have been derived from geophysical mapping techniques, flow and temperature surveys and radioactive tracer experiments.

The graphs of SO_4^{2-} , Cl^- and HCO_3^- concentrations and solution conductivity vs time shown in Fig 11-3 illustrate the general behavior of the reservoir during the 75-day test. Samples taken early in the test have high concentrations of dissolved species (TDS~3300 ppm) and represent undiluted fluid contained in the reservoir several months prior to this experiment. Relatively fresh makeup water (~400 ppm TDS) is injected into the reservoir where it mixes with and dilutes the fluid contained in the fracture system. Initially, when the makeup water rate is high, the dilution effect dominates and concentrations are low. As recirculation continues and the water loss rate to permeation decreases, the concentration of dissolved material rises and eventually approaches an asymptote. The sharp peak on day 23 corresponds

to a sudden change in flow impedance, a short shutdown and a resulting partial flow back of fluid (see Fig. II-1). Water which had been forced into the rock pores returned to the circulating system because of a transitory pressure decline, providing a source of high concentration fluid. As the system returned to its initial injection pressure, the fluid which returned from the pores was replaced and high makeup flows were required. The dilution effect of this high makeup rate is seen for 10 to 15 days in the SiO_2 concentration vs time graph (Fig. 11-3).

Assuming quartz-controlled saturation of SiO_2 in solution, the asymptotic value of SiO_2 concentration shown in Fig. 11-3 suggests a reservoir temperature of 188°C .² The temperature of the water leaving the fracture system and entering the wellbore was measured downhole. Within three days of circulation this downhole temperature was below 160°C corresponding to a quartz-controlled saturation concentration of less than 147 ppm. Clearly the declining mean reservoir temperature could not account for the increasing SiO_2 content in the fluid. A secondary flow path at the initial reservoir temperature is required. According to a simple kinetic model, the change in silica concentration with time for that fraction of the flow corresponds to a first order rate depending on the difference between the silica saturation value of the highest reservoir temperature in contact with flowing fluid and the average silica concentration at any particular time:

$$\frac{d(\overline{\text{SiO}}_2)}{dt} = ka^* \left(\text{SiO}_2_{T=T_{\max}}^{\text{sat}} - \overline{\text{SiO}}_2 \right) \quad (\text{II-1})$$

where ka^* is a constant which includes relevant mass transfer rates, dissolution kinetics rates, and a rock surface area to fluid volume parameter. Assuming no dissolution or reprecipitation occurs in the cooler main flow path, a differential material balance shows that the rate of accumulation of SiO_2 is due to three principle effects: the relative volumes of each flow path, the fluid loss rate due to permeation, and the production of SiO_2 due to active dissolution and/or displacement in the hot region. If the circulation time is large compared to the overall mean residence time τ , the material balance is written as:

$$V \frac{d\bar{C}}{dt} = \dot{q}_T (C_{in} - \bar{C}) + \dot{q}_2 (1 - e^{-ka^* \tau_2 f}) (C^\infty - C_{in}) \quad (11-2)$$

where

$$C_{in} = \frac{\dot{q}_T - q_{loss}}{\dot{q}_T} \bar{C} + \frac{q_{loss}}{\dot{q}_T} C^M$$

$$\begin{aligned} V &= \text{total volume of primary and secondary flow paths} = V_1 + V_2 \\ C^M &= (\text{SiO}_2) \text{ makeup} = \text{concentration of SiO}_2 \text{ in the makeup water} \\ C^\infty &= (\text{SiO}_2)_{\text{sat}} \quad T = T_{\text{max}} = \text{quartz controlled saturation concentration of} \\ &\quad \text{SiO}_2 \text{ at } T_{\text{max}} \end{aligned}$$

$$\begin{aligned} \bar{C} &= (\text{SiO}_2) = \text{average concentration of SiO}_2 \text{ at time } t \\ k_* &= \text{dissolution mass transfer coefficient, cm/sec} \\ a &= \text{rock surface area to fluid volume ratio, cm}^{-1} \\ \dot{q}_2 &= \text{fluid circulation rate through hot region at time } t \\ \dot{q}_T &= \text{total fluid circulation rate at time } t \\ \dot{q}_{loss} &= q_{makeup} = \text{fluid loss rate to permeation at time } t \\ \tau_2 &= \text{mean residence time in hot region (secondary flow path)} \\ f &= \text{fraction of plug flow conversion} = \text{function of dispersion in hot} \\ &\quad \text{region (} f < 1 \text{)} \end{aligned}$$

In the case of low water loss and rapid reaction in the hot region ($ka^* \tau_2 f \gg 1$), eq (II-2) reduces to

$$C_0 e^{-\zeta t} = C^\infty (C^\infty - C_0) e^{-\zeta t} \quad (\text{II-3})$$

The solution to this equation with $\zeta = .04 \text{ sec}^{-1}$, $C^\infty = \text{SiO}_2_{T=180^\circ\text{C}}^{\text{sat}} =$

220 ppm SiO₂ and $C_0 = \text{SiO}_2_{\text{initial}} (t=0) = 80 \text{ ppm}$ (the SiO₂ concentration of the

Initial EE-1 injected water, is shown as the dotted line on the SiO₂ plot of Fig. 11-3. Rate equations of the same form were applied to the fluoride, sulfate and the ^{87/86}Sr data with the same success. Remarkably, the value of ζ is in each case 0.04. Since in all probability more than one mineral is dissolving to contribute SiO₂, SO₄²⁻, F⁻ and Sr to the solution, it would

be quite fortutious that all dissolution rates were equal. Thus it appears that mass transfer rates, specifically mixing rates between various flow fractions, control the concentration history of these particular species in solution.

The possibility remains that saturated pore fluid is merely being displaced from the hot region at a rate q_2 . Further investigation is underway to consider the difference between active dissolution and pore fluid displacement by examining the time dependence of ratios of various ions including Na^+/K^+ / Li^+/Cs^+ and $\text{Cl}^-/\text{Br}^-/\text{I}^-$.

As seen in Fig. 11-3 chloride concentrations also show a marked increase in time possibly indicating displacement and/or mixing with saturated pore fluid because no solid mineral source of chloride should exist at the reservoir conditions. In addition, the rate of increase of Cl^- agrees with the empirical model proposed to explain SiO_2 buildup if a constant concentration source of Cl^- is being supplied to the flow path through the hot region.

In the case of the calcium and bicarbonate concentrations vs time, different conditions prevail (see Fig. 11-3). Calcite (CaCO_3) -- the principal contributor of $\text{CO}_3^{=}$ in solution -- has a retrograde solubility with temperature at a constant CO_2 partial pressure. Therefore, the lowest temperature of the reservoir may control the bicarbonate dissolution, and this lowest temperature is encountered in the main flow path as shown by temperatures measured at the EE-1-to-fracture system connection. In the first 35 days of the run the calcite solubility appears to be controlled by the temperature of the mixed production flow in GT-2B. During the last 40 days, however, the bicarbonate concentration approaches a saturation value corresponding to the calculated EE-1 injection temperature. At least one strong possibility for the apparent shift in control of the calcite solubility to the EE-1 injection temperature is the major change in downhole impedance and a doubling of the EE-1 flow rate that was observed during this period.

Calcium concentrations in equilibrium with calcite and (HCO_3^-) were calculated from the thermodynamic data (equilibrium constants from Garrels and Christ)³ assuming unit activity coefficients. Graphs of Ca^{++} in ppm corresponding to values of HCO_3^- at the GT-2 production temperature are also plotted in Fig. II-3. Notice that the calculated Ca^{++} based on observed

HCO_3^- approaches the Ca^{++} observed at day 45. Until that time, however, the Ca^{calc} is much higher than the Ca^{obs} . Assuming that all the HCO_3^- originally came from calcite, the observed Ca^{++} is an order of magnitude too low during the first 25 days of operation. This could be the result of precipitation of a noncarbonate Ca rich mineral such as phillipsite $(\text{K}_2\text{Na}_2\text{Ca})(\text{Al}_2\text{Si}_4)\text{O}_{12} \cdot 4-5 \text{H}_2\text{O}$. (See ref. 1 for details.)

The discussion above serves to illustrate the complex relationships that exist between the geometric, thermal, and chemical properties of the fracture system. We have been motivated toward selecting simple models and testing their consistency rather than adding unwarranted complexity to improve their fit to the data.

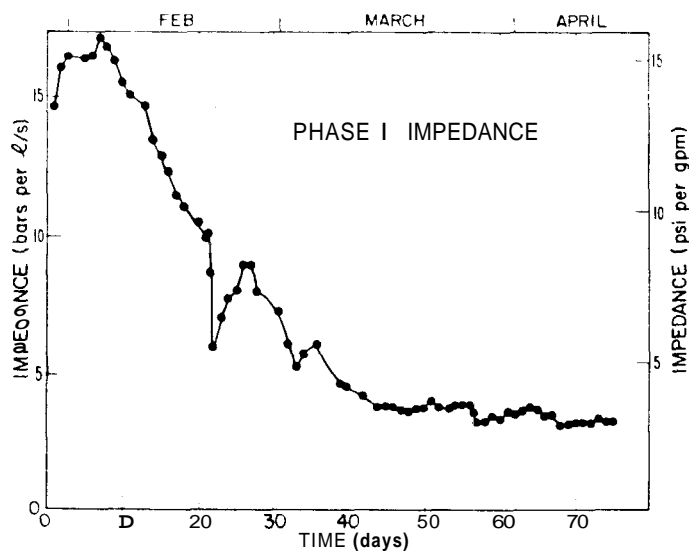


Figure II-1. Net flow impedance between the GT-2B production and EE-1 injection wellbores with buoyancy corrections included.,

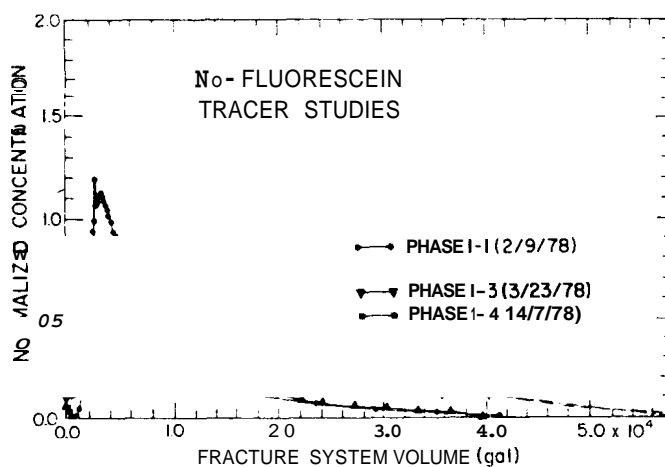


Figure II-2. Normalized tracer concentration as a function of fracture system volume.

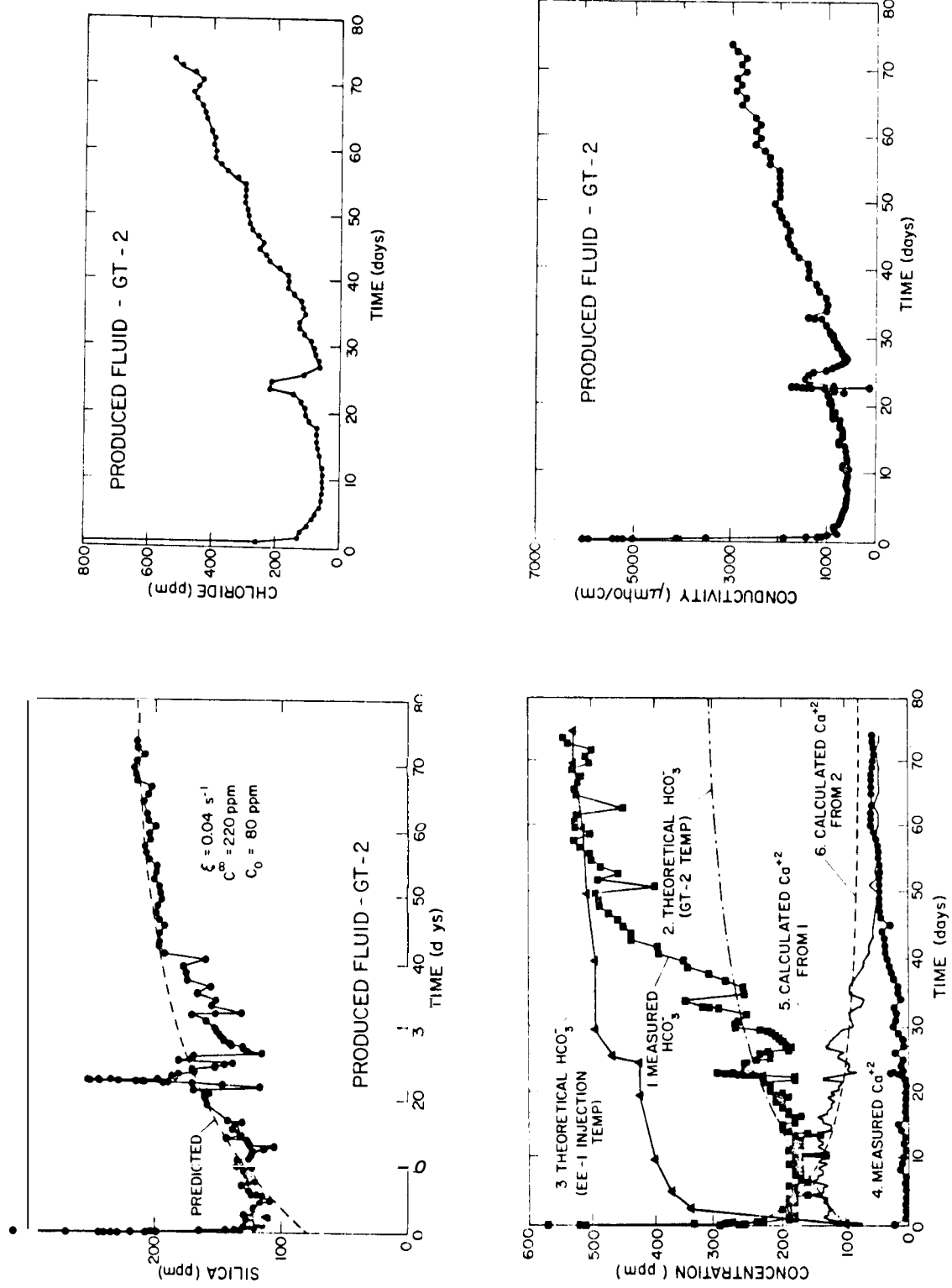


Figure II-3. Concentration histories of dissolved silica (SiO_2), chloride (Cl^-), calcium (Ca^{+2}), and bicarbonate (HCO_3^-) and electrical conductivity of the fluid produced at the GT-2B wellhead during the 75-day Phase 1 test.